A non-contact technique for evaluation of elastic structures at large stand-off distances: applications to classification of fluids in steel vessels

Gregory Kaduchak *, Dipen N. Sinha, David C. Lizon, Michael J. Kelecher

Los Alamos National Laboratory, Electronic and Electrochemical Materials and Devices Group, Los Alamos, NM 87545, USA

Abstract

A novel technique for non-contact evaluation of structures in air at large stand-off distances (on the order of several meters) has been developed. It utilizes a recently constructed air-coupled, parametric acoustic array to excite the resonance vibrations of elastic, fluid-filled vessels. The parametric array is advantageous for NDE applications in that it is capable of producing a much narrower beamwidth and broader bandwidth than typical devices that operate under linear acoustic principles. In the present experiments, the array operates at a carrier frequency of 217 kHz, and the sound field several meters from the source is described spectrally by the envelope of the drive voltage. An operating bandwidth of more than 25 kHz at a center frequency of 15 kHz is demonstrated. For the present application, the array is used to excite vibrations of fluid-filled, steel containers at stand-off distances of greater than 3 m. The vibratory response of a container is detected with a laser vibrometer in a monostatic configuration with the acoustic source. By analyzing the change in the response of the lowest order, antisymmetric Lamb wave as the interior fluid loading conditions of the container are changed, the fluid contained within the steel vessel is classified. © 2000 Published by Elsevier Science B.V. All rights reserved.

1. Introduction

Traditionally, ultrasonic non-destructive testing techniques require direct contact of an acoustic transduction device to excite the vibrational modes of the structure under evaluation. Likewise, direct contact of a receiving mechanism is required to measure the response of the object. These requirements are somewhat lessened by immersing the structure in a highly sound conducting fluid or propagating an acoustic disturbance through a jet of fluid (jet probes). Though these techniques are very robust and efficient in a large number of applications, there are still many situations where direct contact or immersion is not feasible.

Recent advances in non-destructive evaluation of materials address this problem. For example, over the past decade, many studies and applications of laser-generated sound [1–3] and electrochemical acoustic transduction devices (EMAT) [4–6] have reached the literature. These techniques are at the forefront of non-contact acoustic testing and demonstrate remarkable promise for current and future applications with certain limitations. For example, EMATs are limited to very short ranges from the object under inspection. Laser-generated sound requires relatively high optical power levels to produce detectable ultrasonic disturbances on large structures, rendering it problematic in situations where the material under evaluation is very delicate.

The purpose of the research presented here is twofold. First, it describes a novel technique for non-contact acoustic evaluation that employs a non-contact acoustic source that is coupled through the air medium. (With the increased interest in producing efficient, air-coupled acoustic transduction devices [7–9,17], it becomes necessary to re-explore air-coupled NDE techniques.) The technique employs an air-coupled acoustic source that

* Corresponding author. Tel.: +1-505-665-9471;
fax: +1-505-665-4292.
E-mail address: kaduchak@lanl.gov (G. Kaduchak)

utilizes the non-linearity of the air medium to demodulate an amplitude modulated acoustic disturbance (parametric array). In contrast to acoustic devices that operate under linear principles, the parametric array is capable of producing narrower beams and much broader frequency bandwidths. (For the present experiments, a bandwidth of greater than 25 kHz at a center frequency of 15 kHz is demonstrated.) This is very advantageous in non-destructive evaluation scenarios since the narrow beamwidth allows for the *selective* insonification of a target at low frequencies. Likewise, the broad bandwidth of the array makes it possible to excite a broad range of vibrational modes. The measurement of the vibrational response of the target is done with a laser vibrometer in a monostatic configuration with the acoustic parametric array.

Second, the application of this technique to fluid-filled containers demonstrates that classification of fluids in sealed metal containers is possible at stand-off distances of more than 3 m by analyzing the resonance response of the container. More precisely, the classification is accomplished by analyzing the propagation characteristics of the lowest order antisymmetric guided wave (a_0 generalized Lamb wave) which is guided by the circumference of the container [10]. The a_0 Lamb wave is in a class of guided waves that exhibit strong flexural vibrations of the container wall. This equates into large radial displacements of the container wall that are readily detectable. Thus, by analyzing the propagation characteristics of the a_0 Lamb wave, it is possible to detect changes in inertial loading on the interior wall of the container, which yields an insight into the identity of the fluid contained within the vessel.

The paper begins with a description of the parametric array in Section 2. This section will include construction details and results demonstrating the performance of the array as an acoustic emitter. Section 3 describes the experiment, which includes the classification of fluids in sealed steel, cylindrical containers by analyzing the spectral response of the a_0 Lamb wave. Section 4 addresses the results and analysis of the experiments in Section 3. This section also describes the fluid–structure interaction manifest in the a_0 Lamb wave on the cylindrical surface and how different loading conditions affect its propagation characteristics. Section 5 concludes the analysis.

2. Air-coupled parametric array

A parametric array produces a broad-bandwidth, narrow-beamwidth acoustic field by utilizing the non-linearity of the host medium. In the process, two finite amplitude sound beams interact to create secondary sound sources that can be viewed as virtual volume sources produced in the interaction volume of the two sound beams [11–14]. Consider a biharmonic sinusoid that is the result of the addition of two coaxial sound beams at frequencies f_1 and f_2. Neglecting contributions from non-linear processes, the primary pressure field is given by (assuming parallel plane waves)

$$
\begin{aligned}
p(t) &= \cos(2\pi f_1 t) + \cos(2\pi f_2 t) \\
&= 2\cos(2\pi(f_1 - f_2)t)\cos(2\pi((f_1 + f_2)/2)t) \\
&= 2\cos(2\pi f_d t)\cos(2\pi f_s t).
\end{aligned}
$$

The non-linear effect of the host medium on the biharmonic wave results in a secondary sound field p_s. On axis, the secondary field has been shown to be proportional to the second derivative of the square of the difference-frequency component of the field [14]

$$
p_s \propto \frac{\partial^2 E^2(t)}{\partial t^2},
$$

where, for the present case, $E(t) = \cos(2\pi f_d t)$. It should be noted that a secondary sound field is also produced that is associated with the sum-frequency. However, for typical applications in air, where absorption rapidly increases with frequency, contributions to the acoustic field from the high-frequency sum-frequency sources rapidly attenuate with propagation distance [15]. In contrast, secondary sound sources operating at the difference frequency produce sound fields that may propagate large distances due to the low values of attenuation at low frequencies. As discussed later, the difference frequency source possesses a broad bandwidth and narrow beamwidth.

The low frequency sound produced by the parametric array has an extremely broad bandwidth (or large range of difference frequency values) because the bandwidth of the excitation transducers scales with their resonance frequency. As a simple example, consider two transducers with center frequency 200 kHz. Given that they can achieve a 20% bandwidth about their center frequency, they may efficiently excite an acoustic disturbance in the frequency range 180 kHz $< f <$ 220 kHz. If used together in a parametric sound source, the excitation frequencies of these transducers may be adjusted to create a frequency sound field in the frequency range 0 $< f <$ 40 kHz. Contrast this to an acoustic source with center frequency 10 kHz. A 20% bandwidth yields an acoustic source capable of sound production in the frequency range of 9 kHz $< f <$ 11 kHz.

The parametric array used in the following experiments is constructed from 48 commercial off-the-shelf (COTS), air-coupled acoustic transduction devices with a resonance frequency of approximately 200 kHz (AirMar model number AT200). A diagram of the array is shown in Fig. 1. The individual transducers are

**48 Air-Coupled Transducers
(Resonance Frequency ~ 200 kHz)**
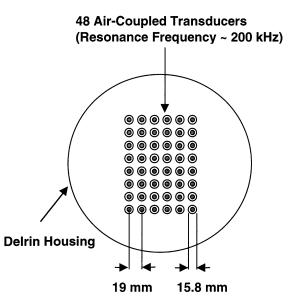

Delrin Housing

19 mm   15.8 mm

Fig. 1. Diagram of acoustic parametric array. It comprises 48 air-coupled transducers with a resonance frequency of 200 kHz and is driven with a biharmonic signal of amplitude 20 V. (The transducers are wired in parallel.) The low-frequency sound generated by the array is described spectrally by the difference-frequency component of the biharmonic field.

mounted in a Delrin housing with approximate 19 mm spacing. The aperture dimension in the horizontal direction is approximately 11.1 cm, and the aperture dimension in the vertical direction is approximately 14.9 cm. The transducers are driven by a KrohnHite model 7602 wideband power amplifier connected to a function generator capable of outputting the product of two sinusoids. The peak-to-peak voltage across each individual transducer is 20 V. For the present application, we are primarily interested in the creation of a secondary sound field at the difference frequency of two closely space frequency components (e.g. $|f_1 - f_2| < 30$ kHz).

The array of transducers is driven with a biharmonic voltage signal described by

$$v(t) = 2 \cos(2\pi f_d t) \cos(2\pi f_s t).$$

Driving one source with a biharmonic signal is equivalent to intersecting the beams of two coaxially located sources operating at frequencies f_1 and f_2, respectively, where $(f_1 + f_2)/2 = f_s$ and $|f_1 - f_2|/2 = f_d$. In the experiments, the sum frequency $f_s = 217$ kHz and difference frequency, f_d, are in the range $2 \, \text{kHz} < f_d < 30 \, \text{kHz}$. Measurements were made of the sound pressure level (SPL) at both the sum and difference frequencies at various locations on axis directly in front of the source. Measurements of the sum-frequency SPL made at a distance of 0.5 m from the array yield a sound pressure level of approximately 115 dB. Several attenuation lengths away (at the target approximately 3 m from the source), measurements of the difference-frequency SPL yield a sound pressure level of approximately 85 dB.

The beam pattern of the array will now be discussed. The difference frequency field is produced along the propagation path of the primary field. The creation of the field is a volume interaction that may be described as a continuous secondary source that extends along the path of propagation of the primary field. The beamwidth of this type of source (similar to an end-fire array) can be extremely narrow relative to a sound field produced by the source aperture operating at the difference-frequency [12,13,16]. This is displayed in Fig. 2. The hollow squares represent experimental measurements taken at a distance of 4 m from the array at the difference-frequency $f_d = 3.9$ kHz. The solid line is the calculated beam pattern for the difference-frequency sound generated by the parametric array used in the experiments. (The calculation is based upon the directivity pattern of a parametric array, which was first derived by Westervelt [11]. See also Refs. [13,14,16].) Finally, the dashed line represents the calculated beam pattern for an aperture of the same dimension driven at the difference frequency. It is obvious from the figure that parametric production of sound displays a much narrower beam pattern than a conventional array of the same aperture size that operates under linear principles.

3. Experimental

The experiment set-up is shown in Fig. 3. The parametric array is placed at a stand-off distance of approximately 3 m from a sealed, steel container. (The container
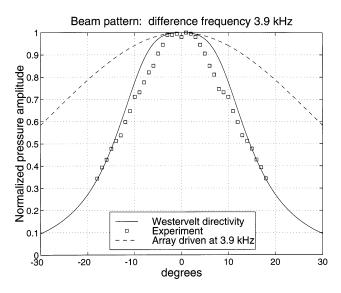

Fig. 2. Directivity pattern for the parametric acoustic array at a difference frequency of 3.9 kHz. Experimental measurements of the difference frequency field are represented by the hollow squares, and the theoretical prediction for a Westervelt-type array is the solid line. The data represented by the dashed line are the directivity pattern for an array of the same dimension driven by a sinusoidal input at the difference frequency.
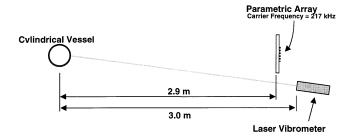
Fig. 3. Experimental configuration for fluid classification in sealed, steel containers. A narrow acoustic beam is generated at the difference frequency of the parametric array. The beam excites the vibrational resonances of the container. (In this case, the vibrational response is due to circumferential resonance of the lowest order antisymmetric Lamb wave on the structure — a_0 Lamb wave.) The vibrational response of the container is measured with a laser vibrometer. By analyzing the shift in the circumferential resonance frequencies of the a_0 Lamb wave as the fluid is changed within the vessel, it is possible to classify the fluid.

is described below.) The container is acoustically excited through the air conduit from this distance over a broad range of excitation frequencies ($2\,\mathrm{kHz} < f_d < 30\,\mathrm{kHz}$) with the array. The container response is measured with a commercial laser vibrometer (Ometron VH300), which is at a similar stand-off distance as the acoustic source. (The laser vibrometer is a Doppler device that measures the velocity of the vibration container wall by detecting the Doppler shift in the reflected light beam. All spectral data shown are thus proportional to the velocity of the vibrating wall.) The spatial resolution of the focused laser beam on the cylindrical surface of the container is approximately 0.5 mm. The output of the vibrometer is passed to a lock-in amplifier that is synchronized with the difference-frequency modulation of the drive voltage. The difference frequency is slowly stepped in 10 Hz increments over the range of modulation frequencies, f_d. It should be noted that the time interval between steps is much greater than the characteristic time to set up circumferential resonances on the container.
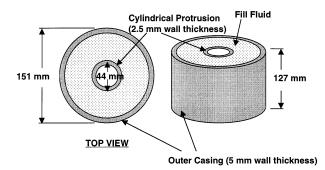

Fig. 4. Steel, fluid-filled containers used in the experiments. Each container has an annular cavity containing either ethylene glycol or isopropanol. It is anticipated that the protrusion in the center of the cavity has a negligible effect on the vibratory response of the external wall of the container.

Table 1
Elastic properties of the vessel

Material	Density (g/cc)	Longitudinal velocity (m/s)	Shear velocity (m/s)
Steel	7.85	5980	3360
Air	0.0012	340	
Isopropanol	0.786	1170	
Ethylene glycol	1.11	1660	

A diagram of the steel container is shown in Fig. 4. It has an outside diameter of 15.1 cm, thickness 0.5 cm and height 12.7 cm. There is a small steel structure protruding from the center of the vessel of diameter 4.4 cm. The approximate elastic properties of the vessel are given in Table 1. (These properties are used in the calculations in Section 4.)

Fig. 5 displays the resonance response of two fluid-filled steel vessels when excited with the parametric array at a stand-off distance of 3 m. The containers are identical except that each is filled with a different fluid: (a) isopropanol and (b) ethylene glycol. (The physical properties for these fluids are listed in Table 1.) The vertical axis of the figure is proportional to the velocity of the vibrating container wall. The horizontal axis refers to the difference-frequency modulation of the transmitted 217 kHz carrier wave. From the figure, it is obvious that the major spectral features (the rather distinct 'spikes') are shifted relative to one another for the two liquid fillers. The frequency shift varies from
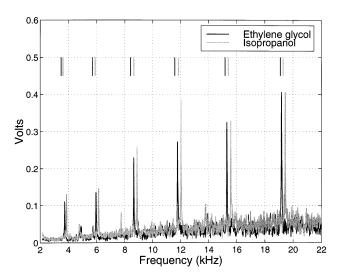

Fig. 5. Spectral response of identical steel vessels containing different fluids. The large, regular peaks correspond to circumferential resonances of the a_0 Lamb wave on the propagating along the circumference of the container. The spectral shifts in the peaks identify different interior loading conditions and thus may be used as a classification tool. The short vertical lines correspond to the locations of the circumferential resonances of the a_0 Lamb wave calculated for an infinite cylinder with the same dimensions and material properties of the cylindrical container in the experiments.

142 Hz near 3.7 kHz to approximately 274 Hz near 19.3 kHz. Experiments confirm that these spectral shifts are not container-dependent. (It should be noted that experiments conducted with the container empty yield spectral shifts of up to 1.2 kHz relative to the ethylene glycol-filled container.)

4. Results and analysis

It is shown in Fig. 5 that the interior fluid loading conditions affect the resonance response of the cylindrical vessel. The resonance frequencies are shifted to slightly lower values for the container with the ethylene glycol filler relative to the isopropanol filled container. This shift is a result of the difference in the interior fluid loading conditions on the internal wall of the container. Increased inertial loading decreases the measured resonance frequencies. This trend is demonstrated in the figure by the downward shift in the resonance frequencies for the vessel containing the 'heavier' ethylene glycol.

Fig. 6 displays the phase velocity of the a_0 Lamb wave calculated for circumferential propagation around an infinite cylinder with the same material parameters as the cylindrical containers described in the experiments above. (See Table 1 for the material properties used in the calculations.) These curves were calculated with the complex mode number methodology of the Sommerfield Watson Transformation for an infinite cylinder externally fluid-loaded by air. (The details of this type of calculation are discussed elsewhere [6].) The black line in the figure displays the normalized phase velocity of the a_0 Lamb wave for interior fluid loading described

Fig. 7. Absolute difference in the phase velocity of the a_0 Lamb wave displayed in Fig. 6. The phase velocity difference accounts for the shifts in the location of the resonant peaks as a function of interior fluid loading of the container.

by ethylene glycol, and the gray line represents the phase velocity of the a_0 Lamb wave for interior fluid loading described by isopropanol. Notice that the phase velocities are slightly different for the two different loading conditions. For clarification, the difference of the phase velocities of the a_0 Lamb wave for the different loading conditions is plotted in Fig. 7.

The circumferential resonance condition for a cylindrical shell is related to the phase velocity of the elastic disturbance

$$f_{res} = \frac{nc_l}{2\pi a} \ (n = 1, 2, 3, \ldots),$$

where a is the radius of the container, c_l is the phase velocity of the disturbance on the cylinder, and n is a positive integer corresponding to the number of full wavelengths required to span the circumference of the vessel [10]. Using the phase velocity values from Fig. 6, the circumferential resonance locations are calculated for the a_0 Lamb wave. The values are shown as the short vertical lines in Fig. 5 for comparison with the experimental data. They demonstrate a good agreement between the measured and calculated values for the resonance frequency locations (and shifts) due to changes in the interior loading conditions.
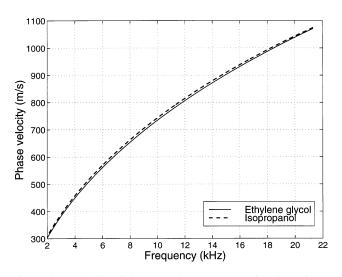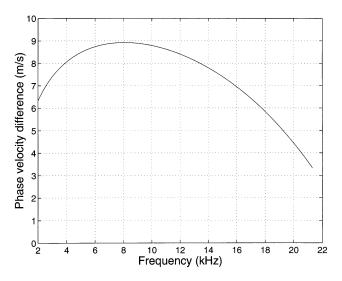

Fig. 6. Phase velocity of the a_0 Lamb wave propagating circumferentially on an infinite cylinder with the dimensions and material properties of the cylindrical container in the experiments. The slight shift in the propagation velocities is the result of different fluid loading conditions on the interior wall of the cylinder.

5. Summary

The research presented above describes a novel technique for acoustic interrogation of elastic structures at large stand-off distances. The technique utilizes a parametric, acoustic array to excite the resonance vibrations

of elastic targets. The non-linear generation of sound yields advantages such as narrower beams for selective insonification of targets and broader bandwidths for increased spectral information.

The array is used to excite cylindrical containers from stand-off distances of more than 3 m. The container response is obtained with a laser vibrometer. Changes in the propagation characteristics of the a_0 Lamb wave on the vessel as a function of the interior fluid loading were demonstrated with filler fluids ethylene glycol and isopropanol. The loading effects of these fluids on the a_0 Lamb wave are easily discernible (and thus the fluids are easily identified) by interrogating the container with the method described above.

Acknowledgement

References

[1] R.D. Huber, R.E. Green, Mater. Eval. 49 (1991) 613–618.

[2] M. Noroy, D. Royer, M. Fink, J. Acoust. Soc. Am. 94 (1934) 1943–1993.

[3] A. Neubrand, P. Hess, J. Appl. Phys. 71 (1992) 227–238.

[4] H. Ogi, J. Appl. Phys. 82 (1997) 3940–3949.

[5] S. Dixon, C. Edwards, S.B. Palmer, Ultrasonics 37 (1999) 273–281.

[6] Z. Guo, J.D. Achenbach, S. Krishnaswamy, Ultrasonics 35 (1997) 423–429.

[7] M.J. Anderson et al., J. Acoust. Soc. Am. 97 (1995) 262–272.

[8] M. Castaings, P. Cawley, J. Acoust. Soc. Am. 100 (1996) 3070–3077.

[9] W.M.D. Wright, D.A. Hutchins, Ultrasonics 37 (1999) 19–22.

[10] N.H. Sun, P.L. Marston, J. Acoust. Soc. Am. 91 (1992) 1398–1402.

[11] P.J. Westervelt, J. Acoust. Soc. Am. 35 (1963) 535–537.

[12] M. Yoneyama et al., J. Acoust. Soc. Am. 73 (1983) 1532–1536.

[13] M.F. Hamilton, in: M.J. Crocker (Ed.), Handbook of Acoustics, Wiley, New York, 1998.

[14] K. Naugolnykh, L. Ostrovsky, Nonlinear Wave Processes in Acoustics, Cambridge University Press, New York, 1998, pp. 165–188.

[15] H.E. Bass, J. Acoust. Soc. Am. 97 (1995) 680–683.

[16] F.J. Fahy, in: M.J. Crocker (Ed.), Handbook of Acoustics, Wiley, New York, 1998.

[17] D.W. Schindel, D.A. Hutchins, Ultrasonics 34 (1996) 621–627.